Canastanes: Ab Initio Quantum Mechanical Prediction of New Curved Polynuclear Aromatic Hydrocarbon Motif

Kim K. Baldridge* and Jay S. Siegel*

San Diego Supercomputer Center
and Department of Chemistry
University of California, San Diego
La Jolla, California 92093-0358

Received October 27, 1998
Revised Manuscript Received March 15, 1999

Graphite serves as the cloth from which several patterns for planar polynuclear aromatic hydrocarbons (PAHs) can be cut. Replacement of six-member rings by five-member rings within the graphitic motif provides the basis for curved PAHs, for example corannulene or fullerene.[1−3] Applying this design principle to carbon-based ribbons yields a series of annelated oligoperilenes that we call [*n*]canastanes in accord with their predicted curved shapes, reminiscent of jai alai baskets (Figure 1). Quantum mechanical computations on this motif reveal several provocative features for $n = 3-5$, **1**−**4**, and these are presented as motivations for the synthesis of this new family of compounds.

Structural computations of the series **1**−**4** were performed at the restricted Hartree−Fock (RHF) level of theory using the analytically determined gradients and search algorithms within GAMESS.[4] Additional hybrid density functional methods (HDFT) were performed using GAUSSIAN94[5] to uncover effects of dynamic correlation. More extensive comparison was done on **1** to determine effects of basis set and correlation. The HDFT methods employed two different exchange correlation functionals, Becke's three-parameter functional[6] in combination with nonlocal correlation provided by the Lee−Yang−Parr expression[7,8] that contains both local and nonlocal terms, B3LYP, and with the nonlocal correlation provided by the Perdew 91 expression,[9] B3PW91. Dunning's correlation consistent basis set, cc-pVDZ,[10] was used for both the RHF and HDFT methods. This basis is a [3s,2p,1d] contraction of a (9s,4p,1d) primitive set. From the fully optimized structures, chemical and physical properties such as ionization potential (Koopman's theorem and ΔSCF),[11,12] dipole moment, bond localization, and surface curvature (carbon pyramidalization)[13−15] were derived. NMR properties at the HDFT level were computed with the CSGT,[16] GIAO,[17,18] and IGAIM[16] methods. We note the relative insensitivity of predicted properties with the inclusion of dynamic correlation as seen for **1** (RHF/cc-pVDZ inversion barrier 2.6 kcal/mol, dipole 1.5 D vs B3PW91/cc-pVDZ inversion barrier 2.4 kcal/mol, dipole 1.3 D). Although a very small basis set places one "in the ballpark" for prediction of barrier height, substantial basis set functionality is necessary to predict higher order properties realistically.

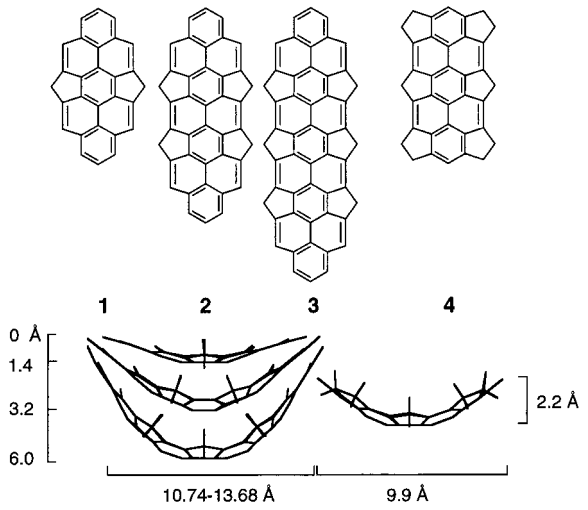

Figure 1. [*n*]Canastanes, **1**−**4**.

Simply adding a five-member ring to a PAH is not sufficient to induce curvature. Numerous "ace-aromatics" aptly prove this point. Therefore, the first order of business is to demonstrate the degree of curvature that one can expect in the canastane series and their resistance to planarization as gauged by their barrier to inversion through a planar state. Along the series **1**−**3**, arc depth increases from 1.35 to 6.06 Å (Table 1). Concomitantly, the relative energy of the planar conformation is exalted from ca. 2.8 kcal/mol in **1** to over 40 kcal/mol in **3** (ca. 44.5 kcal/mol, B3PW91/cc-pVDZ). By adding cyclopenteno annelations to the ends of **1**, one arrives at **4**. The question arises as to the relative importance of additional benzene rings vs additional five-member rings. **4** displays a substantially greater bowl character than **1**, but not to the full extent of **3** (cf. Table 1).

Analysis of the pi bond lengths in **1**−**4** depicts the structure as a polyphenylene core with a small amount of isolated double bond character in the flanking bonds as in pyrene. The vast majority of pi bond lengths are standard benzenoid, 1.40 ± 0.01 Å (1.375 shortest, 1.444 Å longest).

Examining the specific pyramidalization of the sp^2 carbons reveals that the atoms of the base of the arc and in the middle of the band suffer the most. A quantitative gauge of this distortion comes from Haddon's POAV angles, which gauges the pyramidality of a given carbon by the magnitude of the angle between the normal vector of the pyramidal base-plane and the C−C bonds; 90° implies that the C−C bond lies in the best plane and the carbon is flat, and C_{60} has POAV values of 101.6°.[13−15] For **1**, all of the carbons adopt a structure only slightly distorted from planarity (POAV = ca. 91°). The POAV values reach 97−98° for the central rings of **2** and **3**, but taper off to <91° for the terminal rings. In **4**, the POAV angles are similar to those of **3**.

(1) (a) Scott, L. T. *Pure Appl. Chem.* **1996**, *68*, 291−300. (b) Seiders, T. J.; Siegel, J. S. *Chem. Br.* **1995**, *31*, 313−316.
(2) Hirsch, A. *The Chemistry of the Fullerenes*; G. Thieme Verlag: Stuttgart, 1994.
(3) Faust, R. *Angew. Chem., Int. Ed. Engl.* **1995**, *34*, 1429−32.
(4) Schmidt, M. W.; Baldridge, K. K.; Boatz, J. A.; Jensen, J. H.; Koseki, S.; Gordon, M. S.; Nguyen, K. A.; Windus, T. L.; Albert, S. T. *QCPE Bull.* **1990**, *10*.
(5) Frisch, M. J.; Trucks, G. W.; Schlegel, H. B.; Gill, P. M. W.; Johnson, B. G.; Robb, M. A.; Cheeseman, J. R.; Keith, T. A.; Petersson, G. A.; Montgomery, J. A.; Raghavachari, K.; Al-Laham, M. A.; Zakrzewski, V. G.; Ortiz, J. V.; Foresman, J. B.; Cioslowski, J.; Stefanov, B. B.; Nanayakkara, A.; Challacombe, M.; Peng, C. Y.; Ayala, P. Y.; Chen, W.; Wong, M. W.; Andres, J. L.; Replogle, E. S.; Gomperts, R.; Martin, R. L.; Fox, D. J.; Binkley, J. S.; DeFrees, D. J.; Baker, J.; Stewart, J. P.; Head-Gordon, M.; Gonzalez, C.; Pople, J. A. *GAUSSIAN94-DFT*, B.1 ed.; Gaussian, Inc.: Pittsburgh, PA, 1994.
(6) Becke, A. D. *J. Chem. Phys.* **1993**, *98*, 5648−5652.
(7) Lee, C.; Yang, W.; Parr, R. G. *Phys. Rev. B.* **1988**, *37*, 785−789.
(8) Miehlich, B.; Savin, A.; Stoll, H.; Preuss, H. *Chem. Phys. Lett.* **1989**, *157*, 200.
(9) Woon, D. E.; Dunning, T. H. *J. Chem. Phys.* **1993**, *98*, 1358−1371.
(10) Dunning, T. H. *J. Chem. Phys.* **1989**, *90*, 1007−1023.
(11) Almlof, J.; Roos, B.; Wahlgren, U.; Johansen, H. *J. Electron. Spectrosc. Relat. Phenom.* **1973**, *2*, 51−74.
(12) Jordan, K. D.; Paddon-Row: M. N. *J. Phys. Chem.* **1992**, *96*, 1188−1196.
(13) Haddon, R. C. *Acc. Chem. Res.* **1988**, *21*, 243−249.
(14) Haddon, R. C. *J. Am. Chem. Soc.* **1990**, *112*, 3385−3389.
(15) Haddon, R. C.; Brus, L. E.; Raghavachari, K. *Chem. Phys. Lett.* **1986**, *131*, 165−169.
(16) Keith, T. A.; Bader, R. F. W. *Chem. Phys. Lett.* **1992**, *194*, 1−8.
(17) Wolinski, K.; Hinton, J. F.; Pulay, P. *J. Am. Chem. Soc.* **1990**, *112*, 8251−8260.
(18) Ditchfield, R. *J. Chem. Phys.* **1972**, *56*, 5688−5691.

10.1021/ja983744+ CCC: $18.00
Published on Web 05/22/1999

Table 1. B3PW91/cc-pVDZ Structural Data for Canastane Series, **1**−**4**

property	**1**	**2**	**3**	**4**
inversion barrier (kcal/mol)	2.4	24.5	44.5	18.7
dipole (D)	1.3	2.5	2.9	3.5
arc depth (Å)	1.35	3.81	6.06	2.19
arc width (Å)	6.84	6.78	6.75	6.78
arc span at rim (Å)	10.74	12.93	13.68	9.94
arc circumference (Å)	11.2	15.4	19.6	11.2
POAV (range)	91	97−98	97−98	97−98
IP (eV)	6.11	5.64	5.38	5.36

Once distorted out-of-planarity, these ribbons drop in symmetry from D_{2h} to C_{2v} and become polar molecules. Although they are pure hydrocarbons, the anisotropic distribution of carbon−hydrogen bonds and π-electrons causes a substantial segregation of electrostatic charge in the molecule. This segregation of charge is responsible for the high quadrupole moment in benzene and many polar features in aromatic-X interactions.[19,20] The base of the arc becomes the negative end of the dipole, and the arc depth determines the length of charge separation. Thus, the dipole moment increases from 1.3 D in **1** to 2.9 D in **3** (B3PW91/cc-pVDZ) and 3.5 D for **4**. Such values are large for pure hydrocarbons.[21]

The orbital properties of the canastanes vary as a function of curvature and extended conjugation. The prediction of IP on the basis of Koopman's theorem and HOMO energy level follows the trend 6.11 to 5.64 to 5.38 eV for **1**, **2**, and **3**, respectively. Delta SCF computation on **1** predicts an IP of 5.8 eV, supporting the use of Koopman's theorem. Investigation of the specific RHF-orbitals on the series **1**−**3** reveals several changes in orbital rankings. HOMO to HOMO-2 in **1** follows the symmetry pattern B2, B1, A2. The B2 orbital descends, whereas the B1 and A2 orbitals ascend in energy from **1** to **3**. As a result, HOMO to HOMO-2 in **3** follow the symmetry pattern B1, A2, B2. The A2 (LUMO) orbital drops in energy and therefore HOMO/LUMO gap is reduced. In **4**, the IP (5.36 eV) tracks with that of **3**; apparently alkyl substitution and curvature play a more important role than the conjugation due to the additional benzene rings.

An added feature of the canastane design is that the methylene groups of the five-member ring annelations bear diastereotopic hydrogens in the curved conformation. These hydrogens are rendered equivalent in the planar form by the process of arc reversal, and therefore, the coalescence behavior of their NMR signals could be used to assess the barrier to inversion experimentally. Symmetry analysis allows the prediction of the number and type of signals in a given NMR spectrum, but in addition, quantitative predictions of NMR chemical shifts for **1**−**4** can be anticipated by implementation of computational methods such as that provided by the GIAO and IGAIM methods (Table 2). Although the former method is more rigorous, only the latter method is computationally feasible for the larger **2** and **3**. To assess the difference between the two methods, GAIO and IGAIM computations on **1** and **4** were performed at the B3PW91/cc-pVDZ level of theory. Specifically, their ^{1}H NMR spectra should display the following signals in a static curved conformation, values correspond to IGAIM [GIAO] (numbers of protons) δTMS[22] **1**: 7.85 [8.56] (2), 7.96 [8.66] (4), 7.64 [8.46] (4), 4.54 [5.85] (2), 3.30 [4.98] (2); **4**: 6.65 [6.74] (2), 3.96 [3.97] (2), 3.13 [3.00] (4), 2.85 [2.89] (4), 2.62 [2.78] (2), 2.37 [2.40] (4), 2.14 [2.27] (4). The IGAIM method consistently predicts higher chemical shifts and larger differences in chemical shift between the central methylene protons, $\Delta\delta$, than does the GIAO method for this series. The overestimation of IGAIM over GIAO at this level of theory ranges from 0.7 (for the upfield 2H protons) to 1.7 ppm (for the downfield 2H protons) in **1**; much smaller deviations are computed for **4**. With this level of imprecision in mind, we make predictions for the larger analogues using the IGAIM method. The aromatic signals from **1** to **3** vary by ca. 0.7 ppm. The $\Delta\delta$ is predicted to increase from 1.1 to 1.7 ppm, for **1**−**3**, respectively. The end annelations in **4** induce the expected shifts in the aromatic protons of the terminal rings due to alkyl substitution, and $\Delta\delta$ (1.3 ppm) is midway between that of **1**−**3**.

Table 2. B3PW91/cc-pVDZ IGAIM ^{1}H Chemical Shifts

1		**2**		**3**		**4**	
calcd	cor[a]	calcd	cor	calcd	cor	calcd	cor
23.23(2)	7.62	23.46(2)	7.37	23.59(2)	7.23	24.12(2)	6.65
23.14(4)	7.72	23.44(4)	7.39	23.60(4)	7.21	26.56(2)	3.96
23.34(4)	7.50	23.62(4)	7.19	23.81(4)	6.98	27.32(4)	3.13
25.92(2)	4.66	27.46(2)	2.97	26.29(4)	4.26	27.57(4)	2.85
26.91(2)	3.57	26.14(2)	4.42	27.72(4)	2.68	27.79(2)	2.62
				27.86(2)	2.53	28.01(4)	2.37
				26.34(2)	4.20	28.22(4)	2.14

[a] Regression line: $31.64-1.034 \times \text{calcd} = \text{obs}$, $R = 0.921$. Number of protons in parentheses. Shifts reported as ppm.[22]

In general, the canastane motif induces curvature to PAH ribbons. Extension of this motif to higher oligomers must lead to a completely circular PAH without additional strain, normalized per ring. Smaller cycles, PAH tori, can be formed at additional energy costs, and such bonding patterns can be seen as the equatorial regions of fullerenes. Beyond cycles, canastane ribbons of sufficient length will coil into spirals and helices, the pitch, stability, and properties of which still need to be explored. Thus, the canastane motif should provide a significant challenge to synthetic and computational methods.

Acknowledgment. This work was funded by the U.S. National Science Foundation (CHE-9628565; ASC-9212619) and the National Biomedical Computational Resource, in part in absentia from UCSD; K.K.B. (Fulbright Scholar) and J.S.S. (Meyerhoff Professor) Weizmann Institute of Science.

JA983744+

(19) Claessens, M.; Palombini, L.; Stein, M.-L.; Reisse, J. *New J. Chem.* **1982**, *6*, 595−601.
(20) Cozzi, F.; Siegel, J. S. *Pure Appl. Chem.* **1995**, *67*, 683−689.
(21) Baldridge, K. K.; Siegel, J. S. *Theor. Chem. Acc.* **1997**, *97*, 67−71.
(22) δTMS values in ppm are calculated relative to TMS from a regression analysis, see: (a) Chesnut, D. B. *Chem. Phys.* **1997**, *214*, 73−79, (b) Baldridge K. K.; Siegel, J. S. *J. Phys. Chem.* **1999**, *103*, 3, in press.